Amano *et al. Energy Mater* 2024;4:400006
DOI: 10.20517/energymater.2023.77

Energy Materials

Mini Review

Open Access

Proton exchange membrane photoelectrochemical cell for water splitting under vapor feeding

Fumiaki Amano[1,*], **Keisuke Tsushiro**[2]

[1]Department of Applied Chemistry for Environment, Tokyo Metropolitan University, Tokyo 192-0397, Japan.
[2]Department of Chemical and Environmental Engineering, The University of Kitakyushu, Fukuoka 808-0135, Japan.

***Correspondence to:** Prof. Fumiaki Amano, Department of Applied Chemistry for Environment, Tokyo Metropolitan University, 1-1 Minami-Osawa, Hachioji, Tokyo 192-0397, Japan. E-mail: f.amano@tmu.ac.jp

How to cite this article: Amano F, Tsushiro K. Proton exchange membrane photoelectrochemical cell for water splitting under vapor feeding. *Energy Mater* 2024;4:400006. https://dx.doi.org/10.20517/energymater.2023.77

Received: 30 Sep 2023 **First Decision:** 10 Nov 2023 **Revised:** 12 Nov 2023 **Accepted:** 1 Dec 2023 **Published:** 8 Jan 2024

Academic Editors: Chunhui Duan, Nicolas Alonso-Vante **Copy Editor:** Fangling Lan **Production Editor:** Fangling Lan

Abstract

This review provides an overview of recent advancements in vapor-fed photoelectrochemical (PEC) systems specifically designed for utilizing water vapor as a hydrogen resource. The PEC system under water vapor feeding utilizes a proton exchange membrane as a solid polymer electrolyte. Additionally, it utilizes gas-diffusion photoelectrodes composed of a fibrous conductive substrate with macroporous structures. Herein, the porous photoelectrodes are composed of n-type oxides for oxygen evolution reactions and used with a Pt electrocatalyst cathode for hydrogen evolution reactions. The topics covered include the conceptual framework of vapor-fed PEC hydrogen production, strategic design of gas-phase PEC reaction interfaces, and development of porous photoanodes such as titanium dioxide (TiO_2), strontium titanate ($SrTiO_3$), tungsten trioxide (WO_3), and bismuth vanadate ($BiVO_4$). A significant enhancement in the PEC efficiency was achieved through the application of a thin proton-conducting ionomer film on these porous photoelectrodes for surface functionalization. The rational design of proton exchange membrane-based PEC cells will play a pivotal role in realizing renewable-energy-driven hydrogen production from atmospheric humidity in the air.

Keywords: Hydrogen production, oxygen evolution reaction, perfluoro sulfonic acid, photoelectrochemistry, polymer electrolyte membrane, solar fuel

INTRODUCTION

Solar hydrogen

To effectively reduce CO_2 emissions while ensuring economic growth, we must shift from current fossil fuel resources to renewable energy sources, such as solar power. Renewable energy plays a crucial role in achieving a sustainable future by providing environment-friendly alternatives to fossil fuels. Water-splitting technology for H_2 production can convert renewable energy into storable and transportable fuel to mitigate the spatial and temporal disparities in supply and demand. Although sunlight, which is abundant yet diffuse in energy density, holds vast potential for large-scale CO_2-free H_2 production, the challenge lies in achieving cost-effectiveness compared to H_2 production via steam reforming of methane. To address this issue, photocatalytic water splitting has been actively investigated as a potentially cost-effective H_2 production technology[1]. However, the solar-to-hydrogen (STH) energy conversion efficiency is still low (approximately 1%) for state-of-the-art photocatalytic systems, and developing a visible-light-responsive photocatalytic system to enhance its efficiency remains a challenge[2]. Photoelectrochemical (PEC) water splitting, which provides high STH energy conversion efficiency, is a promising technology for solar energy capture and utilization[3,4]. This method has great potential for reducing the reliance on traditional energy sources and mitigating environmental impacts. In this review, we discuss a gas diffusion oxide photoelectrode system supported by surface functionalization using a perfluorosulfonic acid (PFSA) ionomer for PEC water vapor splitting under gas-phase conditions. This system is sustained by polymer electrolyte membranes without the use of liquid aqueous electrolytes.

Humidity in the air as a hydrogen source

Countries facing limitations in domestic renewables have to import chemical energy carriers derived from renewables. For example, the annual solar radiation in Japan is 1,200-1,500 kWh m^{-2}, but arid regions, such as Saudi Arabia and Australia, have abundant solar energy of 2,000-2,100 kWh m^{-2} [Figure 1A]. Because the energy demand in these solar-abundant regions is low, there are opportunities to produce energy carriers for export.

Hydrogen is the primary candidate for solar fuel owing to its chemical simplicity, despite its energy-efficient transportation posing a challenge. Water is a promising electron source for producing energy carriers from renewable sources. However, regions with abundant solar radiation can face challenges regarding freshwater availability, which can become a global issue in the future[5]. To produce H_2 from seawater and wastewater, desalination and purification are required to eliminate impurities poisoning the catalyst, photoelectrode, and membrane. However, the water treatment is both energy-intensive and costly. The use of liquid water also brings about issues such as gas bubble formation, the need for pumping, freezing in low temperatures, and the leaching of toxic components.

One approach to address this challenge involves tapping into atmospheric humidity as an alternative source for hydrogen production. The relative humidity (RH) at the sea surface is consistently high (approximately 80%) throughout the year[6]. Additionally, a recent study indicated that even in arid regions, low concentrations of atmospheric moisture can be condensed into liquids using water adsorbates, thereby facilitating water electrolysis[5]. Several researchers have reported solid polymer electrolyte-based PEC systems, such as membrane-based artificial photosynthetic systems[7,8]. Water vapor splitting using particulate photocatalysts has also been investigated owing to its several advantages over liquid water-based processes, such as easy scalability and suppression of the leaching of catalyst components[9-13].

The use of water vapor has the potential advantage of reducing maintenance costs because the risk of corrosion and poisoning is reduced as water is purified through vaporization. In addition, liquid-pumping

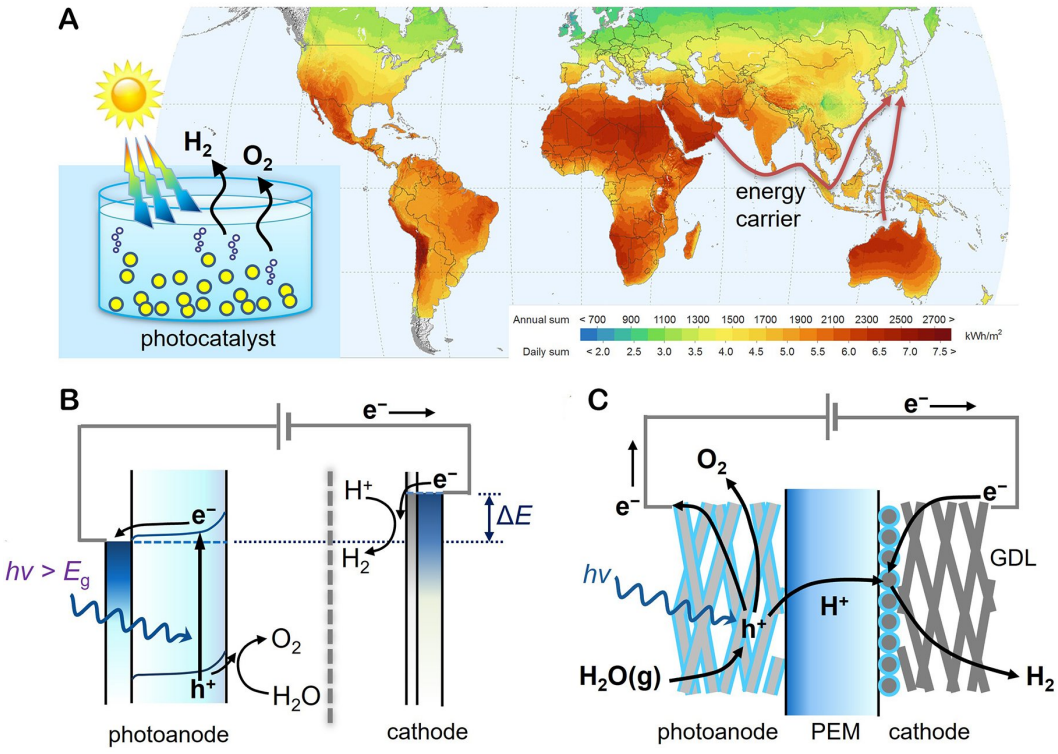

Figure 1. (A) Global distribution of solar radiation on the surface of the Earth (©2020 The World Bank, Source: Global Solar Atlas 2.0, Solar resource data: Solargis) and energy transport to Japan. (B) Schematic of PEC water splitting using a photoanode and cathode immersed in a liquid electrolyte. (C) Schematic of a vapor-fed PEM-PEC system utilizing a porous photoanode and cathode with gas diffusion layer. (B and C) were reproduced from ref.[13].

systems are not required because the natural convection of air can feed water vapor, and the risk of freezing is minimized. The vapor-fed PEC water splitting avoids the deleterious effects associated with bubble formation in aqueous media, the reduction of the contact area between the liquid and electrode, and the reflection and/or scattering of incident illumination[14].

Photocatalysis and photoelectrochemistry

There are two primary categories of solar water-splitting devices, namely hybrid systems combining photovoltaic solar cells with a water electrolyzer and particulate photocatalyst[1-4] PEC systems that fall between these two approaches. Particulate photocatalysts and oxide photoelectrode systems are potential cost-effective routes for scalable hydrogen production. During photocatalytic water splitting, a mixture of H_2 and O_2 gases is produced, which requires membrane separation in the later stages. In contrast, in PEC reactions, pure H_2 is obtained because a membrane separates the gases evolved at the anode and cathode [Figure 1B]. Moreover, an applied external bias or p-n junction can create a potential gradient within the light-responsive semiconductor electrode to enhance charge separation, thereby improving the internal quantum efficiency.

The Honda-Fujishima effect, which involves pairing a titanium dioxide (TiO_2) photoanode with a platinum cathode, is common in PEC systems[15]. An n-type semiconductor can serve as a photoanode for oxygen evolution reactions (OERs), while a p-type semiconductor can serve as a photocathode for hydrogen evolution reactions (HERs). The tandem combination of an oxide photoanode with a photocathode allows for the utilization of narrow bandgap semiconductors through two-step photoexcitation. In conventional

water electrolysis, the overvoltage of the OER at the anode surpasses that at the HER cathode. This emphasizes the significance of developing photoanode materials for the OER. Oxide semiconductors are often favored as O_2-evolving photoanodes because of their resistance to photocorrosion.

When a photoanode is exposed to light with energy surpassing its band gap (*E*g), photoabsorption generates holes (h^+) in the valence band, leading to oxygen production via four-electron water oxidation ($2H_2O \rightarrow O_2 + 4H^+ + 4e^-$). These PEC reactions typically occur on semiconductor electrodes immersed in aqueous electrolyte solutions. However, the limited availability of freshwater poses challenges in upscaling hydrogen production. Hence, researchers have investigated PEC systems in which water vapor (gaseous phase) acted as the reactant [Figure 1C]. A proton exchange membrane (PEM) was used as the solid electrolyte, with water supplied in vapor forms. In the PEM-PEC devices, it was difficult to integrate conventional photoelectrodes fabricated on two-dimensional substrates, such as sheets and plates, owing to the ion transport limitations toward the membrane. The semiconductor electrodes must exhibit porosity to facilitate the diffusion of water vapor and evolving oxygen, along with proton transport to the counter electrode through the electrode and membrane.

Historical overview of PEM-PEC devices

The PEM-PEC cell design minimized the gap between the two electrodes to reduce the electrolyte resistance and prevent the mixing of the gases evolved at each electrode. In 1996, Ichikawa reported the first PEM-PEC cell with a perforated thin film of anatase TiO_2 and an electrocatalyst separated by a Nafion membrane[16]. The TiO_2 photoanode facilitated liquid water oxidation, generating dioxygen and protons. These protons then move to the Pt and ZnO/Cu electrocatalysts for H_2 production and CO_2 reduction, respectively. In 2009, Seger and Kamat reported a PEM-PEC cell consisting of an anatase TiO_2 photoanode and Pt cathode for H_2 production[17]. They achieved the methanol solution oxidation using TiO_2 nanoparticles (Degussa P25) on carbon paper under UV irradiation without an external bias voltage. Later, several groups applied PEM-PEC systems for splitting water using a KOH solution or electrolyte-free pure water[18-20].

For gas-phase reaction, Georgieva *et al.* first applied a PEM-PEC cell for the photooxidation of methanol vapor in air under UV and visible light illumination in 2009[21]. They observed an increase in the photocurrent of TiO_2/tungsten trioxide (WO_3)-coated stainless steel with increasing gaseous methanol concentration when exposed to air streams saturated with water and methanol vapor. Iwu *et al.* reported PEC oxidation of gaseous methanol and water vapor using a TiO_2 P25 photocatalyst on carbon paper[22]. In 2014, Rongé *et al.* demonstrated a PEM-PEC cell that produced hydrogen from the water vapor present in the air[23]. The PEC oxidation of water vapor was facilitated over TiO_2 thin films coated multi-walled carbon nanotubes that were grafted onto carbon fiber felt, the surface of which was functionalized with a thin PFSA film and water-adsorbing zeolite particles. The key materials to achieve PEC water vapor splitting included photoanodes fabricated on carbon fibers and stainless steel mesh.

This mini-review introduces the development of porous photoanodes that utilize titanium felt as a conductive substrate, focusing primarily on our research efforts[13,24-28]. The recent progress in the vapor-fed PEM-PEC cell is presented based on the rational design of the gas-diffusion oxide photoanodes and the triple-phase boundary concept under the gas-phase conditions. Finally, suggestions for future work are provided to improve the STH energy conversion efficiency of the PEM-PEC cell.

VAPOR-FED PEC HYDROGEN PRODUCTION

Porous tungsten trioxide photoanode

In polymer electrolyte fuel cells, waterproofed carbon fibers (commonly known as carbon paper) typically serve as gas-diffusion layers. Because of concerns regarding the potential oxidative degradation of carbon during the photoanode reaction, titanium fiber felt was opted for the conductive substrate for porous tungsten oxide (WO_3) electrodes. Amano *et al.* prepared the WO_3 layer on three-dimensional macroporous titanium fibers through a dip-coating method and subsequent calcination[29]. The titanium felt was soaked in an aqueous precursor solution of ammonium metatungstate, including polyethylene glycol. Then, the precursor-coated felt was calcined in air at 650 °C for 1 h to obtain the porous WO_3 electrode. Titanium has superior thermal durability in oxidizing atmospheres compared to conventional transparent conductive oxide substrates[30].

Figure 2A shows the scanning electron microscopy (SEM) images of the WO_3 electrode prepared using titanium felt as the conductive substrate (porosity: 66.6%)[24]. The titanium fibers, with a converted diameter of 20 μm, were uniformly coated with a WO_3 layer to maintain substantial porosity ranging from several tens of microns to several microns. The WO_3 layer was composed of fine particles of diameters of ~100 nm, forming pore spaces that were several tens of nanometers in size. The bimodal porous WO_3 electrode exhibited good photoanodic properties in aqueous electrolyte solutions[29]. The preparation of porous WO_3 photoanodes using carbon microfiber felt as a conductive substrate has also been reported[31,32].

Triple-phase boundary for gas-fed PEC reaction

The fabricated gas-diffusion WO_3 electrode was attached to the PEM (Nafion 117 membrane) to create a membrane electrode assembly [Figure 2B]. A carbon-supported Pt electrocatalyst was used as the cathode in polymer electrolyte fuel cells. The membrane electrode assembly was then placed in a homemade electrolyzer equipped with an optical window, establishing the PEM-PEC cell. Approximately 3 vol% water vapor at ~90% RH and 25 °C was supplied to each of the two electrodes by bubbling argon at a flow rate of 20 mL min^{-1} into deionized water. The irradiation area of the photoanode was 16 cm^2, and a blue light-emitting diode (LED) with a central wavelength of 453 nm was used as the light source [Figure 2B]. The irradiance was 7 mW cm^{-2} at 453 nm. The temperature of the PEM-PEC cell slightly increased by 2 °C during light irradiation, and the experiment was conducted under conditions that did not lead to water vapor condensation.

The photocurrent response of WO_3 electrodes in a water vapor environment is shown in Figure 3[25]. When utilizing an all-solid-state PEM-PEC cell, the photocurrent response is significantly lower than that in an aqueous electrolyte solution. To address this, a proton-conducting PFSA ionomer dispersion was applied to the WO_3 electrode and subsequently dried at 80 °C to form a thin ionomer film on the surface. While the uncoated WO_3 electrode demonstrated poor performance, the ionomer coating significantly enhanced the photocurrent response in a water vapor atmosphere [Figure 3A]. This indicates that surface functionalization is required to improve the proton conduction across the porous photoanode and membrane.

Gas chromatography confirmed oxygen production at the porous WO_3 photoanode under vapor-feeding conditions [Figure 3B]. With the ionomer coating, the Faradaic efficiency (FE) of O_2 generation was 80%, indicating effective progress in water splitting. In contrast, the O_2 FE before surface coating was low, indicating that the OER did not proceed easily in the gas-phase environment. Unlike in an aqueous electrolyte solution, proton-coupled electron transfer, involving proton transport, is the rate-determining step in OERs [Figure 3C].

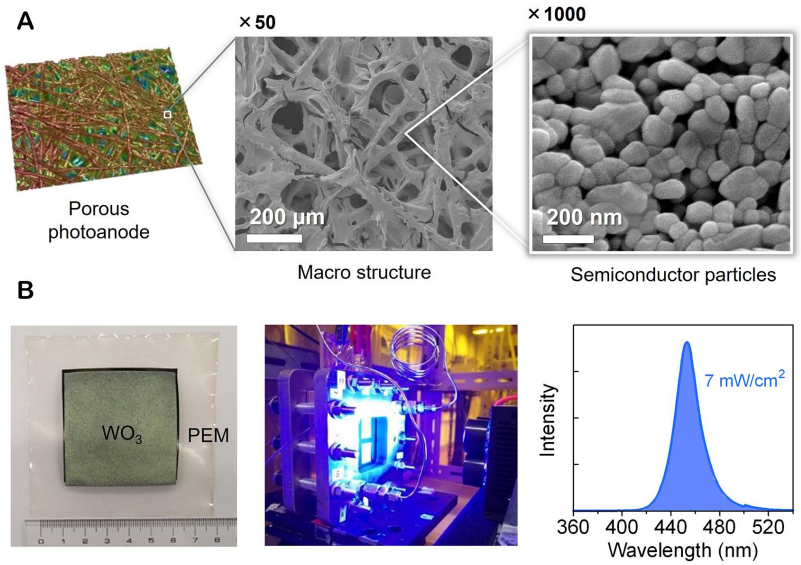

Figure 2. (A) Macroporous and microporous structure of gas-diffusion WO_3 electrodes. (B) Membrane electrode assembly with an electrode area of 25 cm^2, a stainless steel PEM-PEC cell with a 16 cm^2 irradiation area, and the spectrum of a blue LED light source for the vapor-fed system (wavelength: 453 nm, irradiance: 7 mW cm^{-2}, and temperature: 25 °C). Reproduced with permission from ref.[24], Copyright 2019, American Chemical Society.

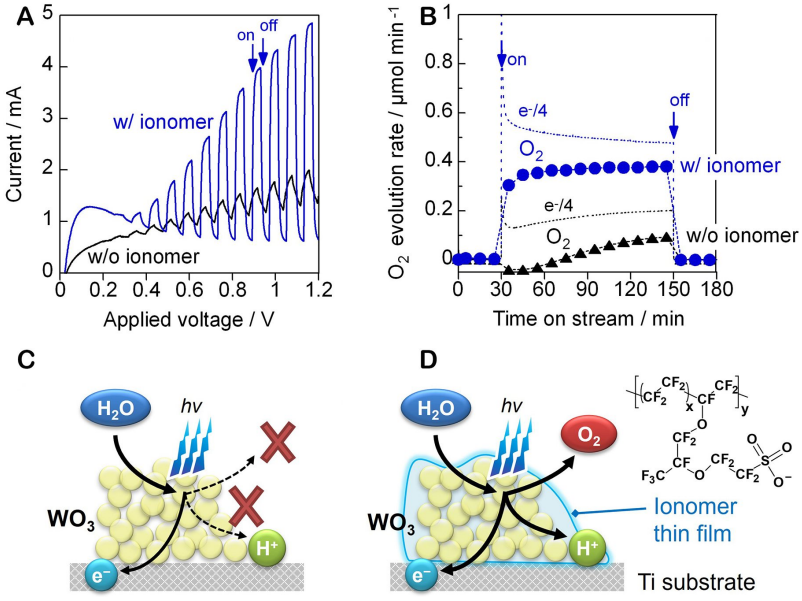

Figure 3. PEC splitting of water vapor using WO_3 photoanode: (A) dependence of photocurrent response on the applied voltage and (B) time-dependent O_2 production rate over the photoanode at an applied voltage of 1.2 V *vs.* cathode (wavelength: 453 nm, irradiance: 7 mW cm^{-2}, and irradiation area: 16 cm^2). Schematic illustrations of the interfacial structure of WO_3 photoanodes in a gas-phase atmosphere: (C) bare WO_3, where proton transport is the rate-determining step and (D) PEC triple-phase boundary formed by a thin PFSA ionomer film coating on the surface. Reproduced from ref.[25], Copyright 2018 Amano *et al.*[25].

However, when a PFSA ionomer film is used for surface functionalization, proton-coupled electron transfer and proton transport are no longer the rate-determining step, even in gas-phase environments without liquid electrolytes. This facilitates a fast multiple-electron transfer pathway, resulting in a good photocurrent response and high O_2 FE [Figure 3D]. In vapor-fed PEC water splitting without an aqueous electrolyte,

integrating processes such as photoabsorption, electron conduction, proton transport, and the diffusion of reactants and products is crucial. The design of a triple-phase boundary, including a "gas phase-electrolyte-semiconductor" boundary, plays a pivotal role in this gaseous PEC process in the absence of liquid water.

Furthermore, the PFSA ionomer and PEM serve as humidity adsorbents in the gas phase. Diffuse reflectance infrared spectroscopy revealed that the PFSA ionomer increased the amount of water adsorbed at low concentrations of water vapor and formed hydronium ions (H_3O^+) with weakly hydrogen-bonded water molecules[13]. The physical properties of water adsorption on semiconductor surfaces have been reviewed[9]. The amount of water adsorbed is closely related to the RH in the system, and the adsorbed water layer affects the proton conductivity and number of contacts between water and the reaction sites. Further research is needed to separate the effects of water absorption in the ionomer and the effects of proton transport.

PEC PROPERTIES OF POROUS SEMICONDUCTOR ELECTRODES

Titanium dioxide electrodes

The insights gained from the porous WO_3 electrode were applied to other semiconductor electrodes, including anatase and rutile TiO_2 electrodes. Anatase TiO_2 electrodes were prepared by electrochemically anodizing titanium fibers in ethylene glycol with 0.25% NH_4F and 10 vol% water at 50 V for 3 h; subsequently, they were crystallized through calcination in air at 550 °C for 1 h[26]. The SEM image of the rectangular-shaped titanium fiber showed a layer of TiO_2 nanotube arrays with an outer diameter, a wall thickness, and a length of 110-140 nm, 15-30 nm, and ~5 μm, respectively [Figure 4A]. Stoll *et al.* also reported the anodization of Ti felt in ethylene glycol with 0.3% NH_4F and 2 vol% water at 30 V for 1 h, yielding TiO_2 nanotube arrays[33]. In the nanotube structure, the photogenerated holes diffused through the wall thickness to the electrolyte interface over a short distance, while the photoexcited electrons were transported along the long axial direction of the TiO_2 nanotubes to the conductive substrate[34].

In a water vapor environment (RH < 100%), the anatase TiO_2 nanotube arrays without ionomer functionalization initially exhibited no photocurrent response [Figure 4B]. Following the surface functionalization by the PFSA ionomer, the photocurrent monotonically increased with each subsequent coating (10 μL cm^{-2} of a 5 wt% dispersion). After the third coating, the incident photon-to-current conversion efficiency (IPCE) remained nearly constant and was comparable to that of TiO_2 nanotube arrays in 0.2 mol L^{-1} sodium sulfate solution (IPCE: 26.5%). This revealed that even under water vapor feeding, an ionomer modification of approximately 1.5 mg cm^{-2} resulted in a performance equivalent to that in an aqueous solution[26].

Figure 5A shows the vapor-fed PEC reaction over an anatase TiO_2 nanotube array photoanode. When an external voltage of 1.2 V was applied, the IPCE was 16% at a wavelength of 365 nm (40 mW cm^{-2}); the UV irradiation area was 16 cm^2, and the H_2 production rate was 600 μmol h^{-1}. The FE of H_2 generation at the cathode was close to 100%; however, the O_2 FE at the photoanode was only 86%, indicating that CO_2 was produced as a byproduct due to the oxidative decomposition of the PFSA ionomer. Energy-dispersive X-ray spectroscopy (EDS) revealed a decrease in the fluorine content on the TiO_2 surface, indicating the degradation of the ionomer during the vapor-fed PEC reaction. Similar results were obtained for the PEC reaction using a rutile TiO_2 electrode under water vapor feeding (RH < 100%)[27]. Under a 385-nm UV illumination, the IPCE of rutile TiO_2 (8.7%) was much higher than that of the anatase TiO_2 nanotube array (4.8%) at an applied voltage of 1.2 V owing to the band gap of rutile (3.0 eV) being narrower than that of anatase (3.2 eV).

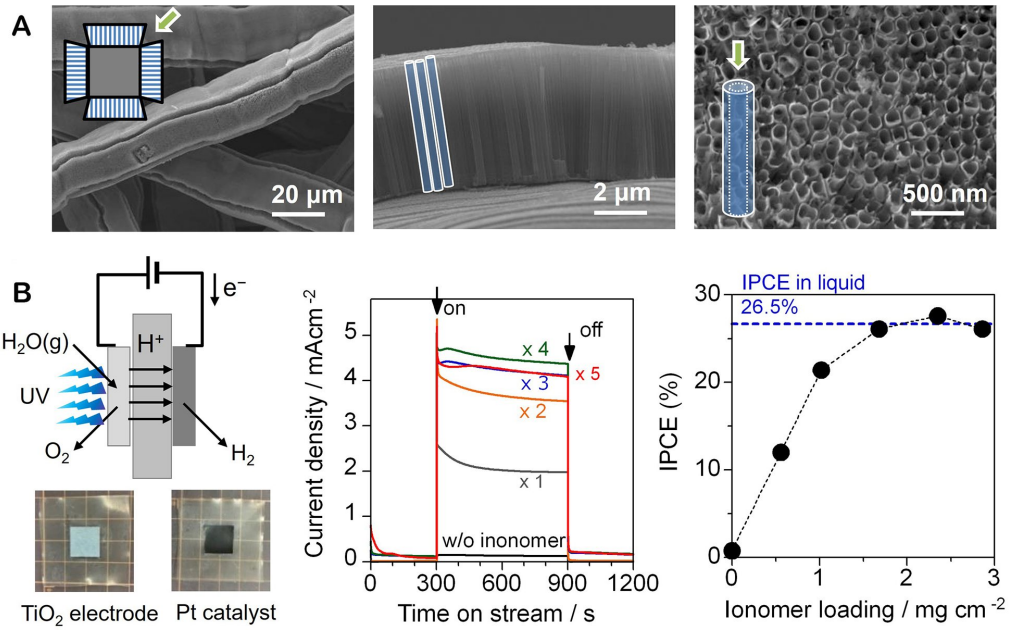

Figure 4. (A) SEM image of the TiO_2 nanotube array formed by anodizing titanium fibers. (B) Membrane electrode assembly used in vapor-fed PEC water splitting in a humidified argon atmosphere (3 vol% H_2O), utilizing TiO_2 nanotube array photoanodes and Pt-carbon cathodes. The effect of PFSA ionomer coating number on their photocurrent response and IPCE at an applied voltage of 1.2 V *vs.* cathode (wavelength: 365 nm, irradiance: 56 mW cm^{-2}, irradiation area: 1 cm^2) has also been included. Reproduced with permission from ref.[26], Copyright 2018 Wiley.

The PEC water vapor splitting reaction under a humidified argon stream exhibited a high H_2 production rate (~600 μmol h^{-1}) at the laboratory level. In practical operations, it is necessary to utilize the humidity in the air [Figure 5B]. To confirm this hypothesis, the carrier gas in the photoanode chamber was switched from humidified Ar to humidified air. However, no difference was observed in the photocurrent response, indicating that water vapor can be oxidatively decomposed, even in the presence of O_2 in air[26]. This finding highlights the potential of utilizing the porous OER photoanodes to harness atmospheric moisture for H_2 production.

Following the studies of our group, Zafeiropoulos *et al.* also reported the functionalization of porous TiO_2 and WO_3 photoanodes with proton-conducting PFSA ionomers (Aquivion and Nafion)[35]. The optimized and functionalized photoanodes operating at 60% RH within a temperature range of 30-70 °C were able to recover up to 90% of the performance obtained at 1.23 V *vs.* RHE in the conventional liquid phase. The bare photoanodes, without ionomer functionalization, did not show a photocurrent response at RH < 100%, whereas Stoll *et al.* previously performed the PEM-PEC reaction under conditions in which water condensed (RH > 100%)[33,36,37]. The photocatalytic water splitting reaction significantly depends on the presence of a condensed water film on the semiconductor surface for proton conductivity between the oxidation and reduction sites[10]. Xu *et al.* reported a PEM-PEC system without ionomer functionalization, where liquid-like water layers formed on the surface of nanostructured TiO_2 in humid air[38,39].

Strontium titanate electrode

Strontium titanate ($SrTiO_3$) is an effective photocatalyst used for water splitting. To prepare $SrTiO_3$ electrodes, the anatase TiO_2 nanotube arrays underwent further treatment by a hydrothermal reaction in 25 mM $Sr(OH)_2$ at 150 °C for 2 h and subsequent calcination in air at 550 °C for 1 h[13]. Despite the collapse of the nanotube structure, particulate structures were obtained, in which the nanoparticles appeared to be

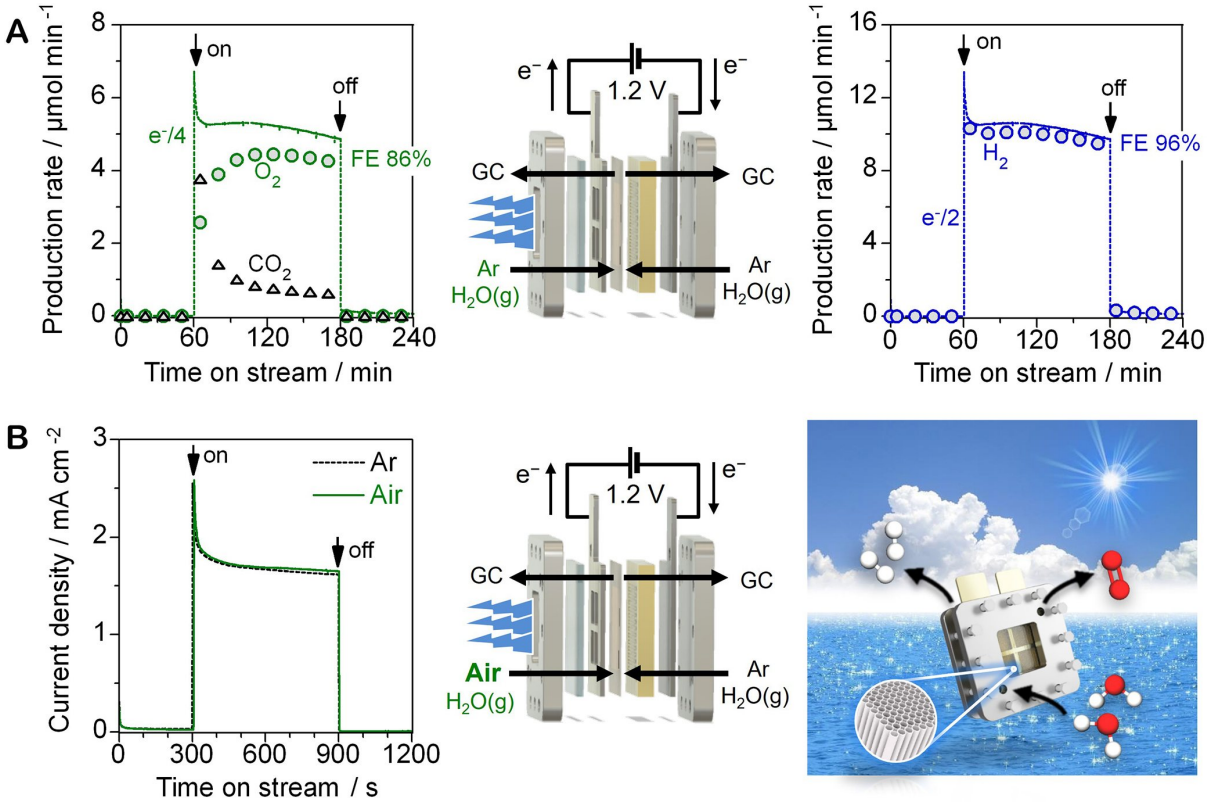

Figure 5. (A) Production rate of O_2 and CO_2 in the photoanodic compartment and H_2 in the cathodic compartment during vapor-fed PEC water splitting under humidified argon flow with a TiO_2 nanotube array photoanode (wavelength: 365 nm, irradiance: 40 mW cm^{-2}, and applied voltage: 1.2 V). (B) Impact of the carrier gas (humidified argon and air) in the photoanode compartment on the photocurrent response of the anatase TiO_2 nanotube array photoanode. Reproduced with permission from ref.[26], Copyright 2018 Wiley.

interconnected to form mesoporous structures [Figure 6A]. The PEC properties of the $SrTiO_3$ electrode, evaluated in a 0.2 M Na_2SO_4 aqueous solution, revealed that the photocurrent onset potential shifted to the lower potential side in comparison to the anatase TiO_2 photoanode [Figure 6B]. This indicates that the PEC water oxidation reaction proceeds with the application of a smaller applied bias. Furthermore, the $SrTiO_3$ electrode exhibited a photocurrent response even at 0.3 V *vs.* RHE, whereas the TiO_2 electrode exhibited no photocurrent under the same conditions [Figure 6C].

Subsequently, PEC properties were evaluated under gas-phase conditions using a photoanode with an irradiated area of 2 cm^2 [Figure 7]. At an applied voltage of 0.3 V, a photocurrent response was observed for the anatase TiO_2 nanotubes and $SrTiO_3$ photoanodes with surface functionalization. H_2 was produced at the cathode with an FE of 100%. However, CO_2 was predominantly produced on the TiO_2 photoanode, indicating that the H_2 evolution is accompanied by the degradation of the PFSA ionomer rather than an overall water-splitting reaction[13]. In contrast, the $SrTiO_3$ photoanode induced the production of H_2 and O_2 at a stoichiometric ratio of 2:1, and the produced CO_2 was undetectable (O_2 FE approached 100%). When utilizing the $SrTiO_3$ photoanode, water vapor completely decomposed into H_2 and O_2, and membrane separation was simultaneously achieved with the application of a small voltage. This is a major feature of the PEM-PEC reaction, which differs from photocatalytic reactions under water vapor feeding.

The durability of the PEM-PEC system was evaluated over 10 h [Figure 8]. Functionalized $SrTiO_3$ photoanodes had a significant advantage in terms of their prolonged operational lifetime[13]. In contrast, for

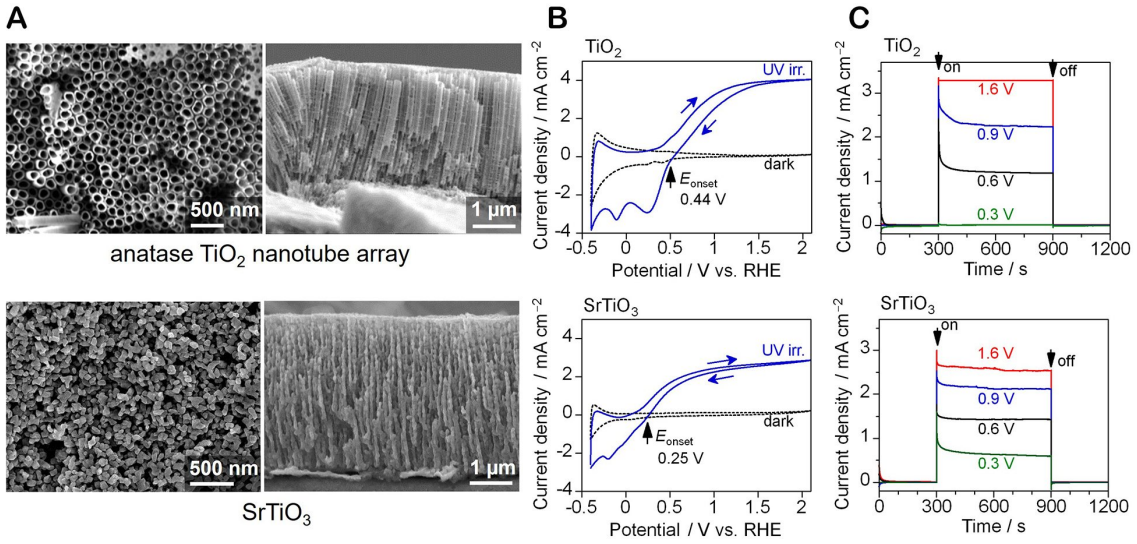

Figure 6. Comparison of anatase TiO_2 nanotube array and $SrTiO_3$ photoanode. (A) SEM images of the top and side views of the oxide layers. (B) Cyclic voltammograms and (C) photocurrent response of anatase TiO_2 and $SrTiO_3$ photoanodes in aqueous 0.2 M Na_2SO_4 and 0.1 M NaPi solution (pH: 6.7, wavelength: 365 nm, and irradiance: 40 mW cm^{-2}) at varying applied potential (V *vs.* RHE). Reproduced from ref.[13] with permission from the Royal Society of Chemistry.

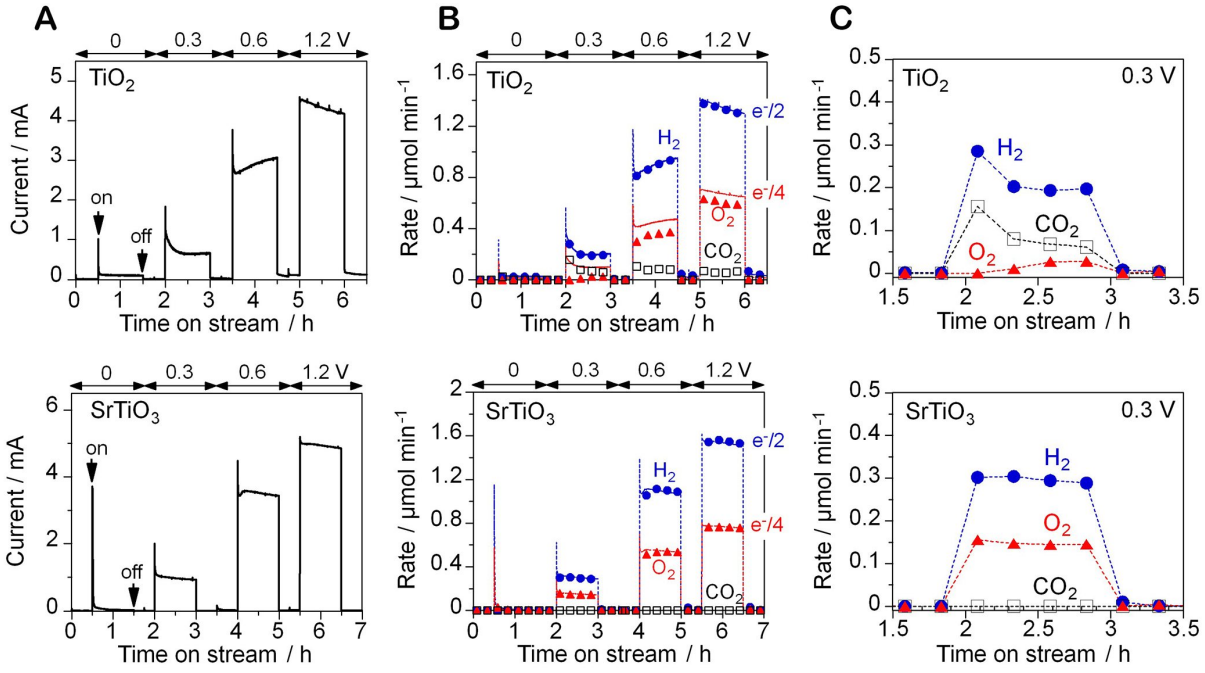

Figure 7. PEC properties of anatase TiO_2 and $SrTiO_3$ photoanodes with an irradiation area of 2 cm^2 in a vapor-fed water splitting system (wavelength: 365 nm and irradiance: 40 mW cm^{-2}). Impact of applied voltage (V *vs.* cathode) on (A) photocurrent response and (B) rate of H_2 formation in the cathode compartment and O_2 and CO_2 formation in the photoanode compartment. (C) Enlarged view of the product formation rate at 0.3 V *vs.* cathode. Reproduced from ref.[13] with permission from the Royal Society of Chemistry.

anatase and rutile TiO_2 photoanodes, the surface ionomer coating responsible for proton transport was degraded under vapor-fed gas-phase conditions, which led to a gradual decrease in the photocurrent. The IPCE gradually decreased to 6.3% for the anatase TiO_2 photoanode. The O_2 evolution rate was lower than

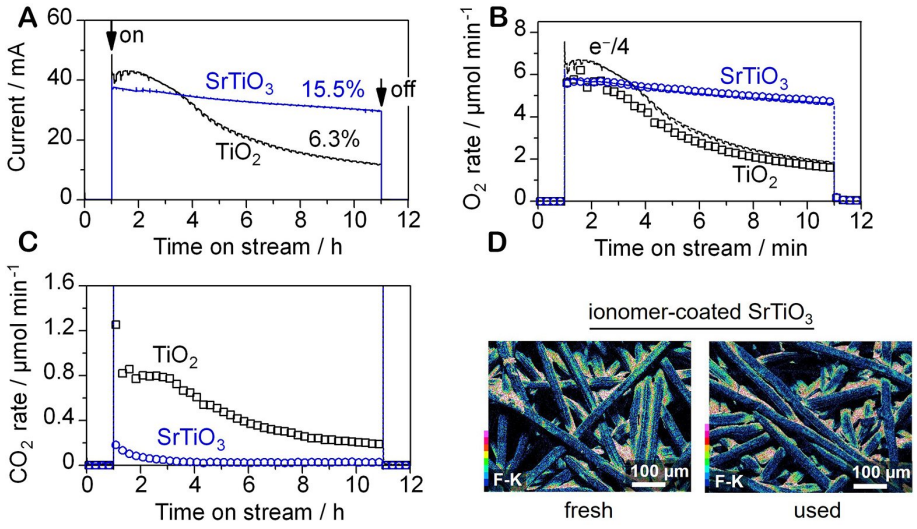

Figure 8. Durability of anatase TiO_2 and $SrTiO_3$ photoanodes in vapor-fed PEC water splitting. (A) Photocurrent response (the numbers in the figure are the IPCE just before the light was turned off), (B) O_2 production rate, and (C) CO_2 production rate (wavelength: 365 nm, irradiance: 40 mW cm^{-2}, irradiation area: 16 cm^2, and applied voltage: 1.2 V *vs.* cathode). (D) SEM-EDS images of fluorine in the ionomer-coated $SrTiO_3$ photoanode before and after the PEC reaction. Reproduced from ref.[13] with permission from the Royal Society of Chemistry.

the rate of one-quarter of the electron transfer ($e^-/4$) owing to the formation of CO_2 from ionomer degradation. The fluorine/titanium (F/Ti) ratio, determined by SEM-EDS analysis, decreased from 1.64 to 0.41 after the vapor-fed PEC reaction, suggesting the degradation of the PFSA ionomer on the TiO_2 photoanode. The oxidative degradation is probably due to the hydroxyl radical generation on the TiO_2 surface. In contrast, the $SrTiO_3$ photoanode exhibited relatively stable photocurrents, maintaining an IPCE of 15.5%, even after a vapor-fed PEC reaction for 10 h. An analysis of the SEM-EDS images indicated that the F/Ti ratio remained constant after the reaction [Figure 8D]. The O_2 FE of $SrTiO_3$ was almost 100%, as confirmed by the O_2 formation rate, which was in agreement with the $e^-/4$ rate, while the CO_2 formation was negligible. The improved reaction selectivity for the OER over $SrTiO_3$ photoanodes increased the lifetime of the PEM-PEC system. A bias-free STH device will be developed by combination with a photocathode or by reducing the applied voltage of the photoanode in the PEM-PEC system.

Bismuth vanadate electrode

Bismuth vanadate ($BiVO_4$) with an E_g of 2.4 eV is recognized as a visible light-responsive photoanode. To enhance the performance of vapor-fed PEC water splitting under visible light irradiation, our group prepared porous $BiVO_4$ electrodes using Ti felt as a conductive substrate by a dip-coating of the precursor solution of $Bi(NO_3)_3$ and $VO(acac)_2$ and subsequent calcination at 500 °C[28]. The photocurrent response of each porous photoanode was investigated in a phosphate buffer solution using a light source (blue LED) with a central wavelength of 454 nm [Figure 9A]. The performance of a single $BiVO_4$ was inferior to that of a single WO_3 (E_g = 2.7 eV), which was also responsive to blue light. When a $BiVO_4$ layer was coated onto the WO_3 photoanode, an increase in the photocurrent was observed. Upon doping Mo species into the $BiVO_4$ layer, the IPCE significantly increased to 10.7%, owing to the increased electron density resulting from the substitution of Mo^{6+} for V^{5+}. Furthermore, the WO_3/Mo-$BiVO_4$ heterojunction photoanode exhibited a photocurrent response at a wavelength of approximately 500 nm, which is longer than that of the WO_3 photoanode [Figure 9B].

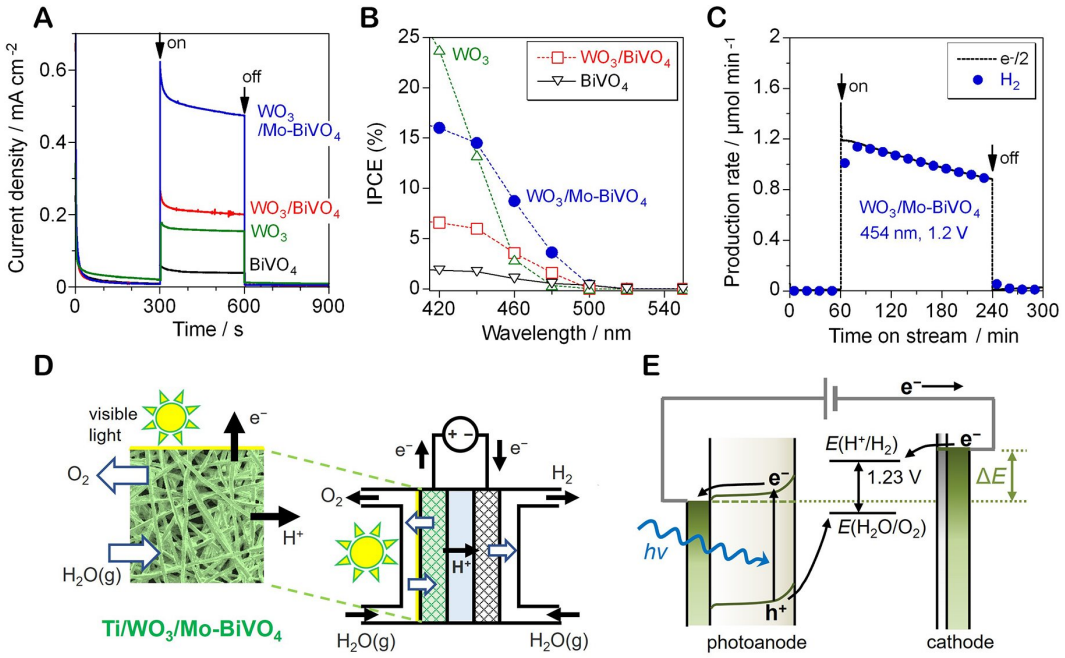

Figure 9. PEC properties of WO_3/Mo-doped $BiVO_4$ photoanodes under visible light irradiation. (A) Photocurrent response under 454 nm irradiation and (B) IPCE action spectra in aqueous 0.1 M NaPi solution at 1.2 V *vs.* RHE. (C) Photocurrent in the vapor-fed PEC water splitting using WO_3/Mo-$BiVO_4$ photoanode at an applied voltage of 1.2 V (light source: blue LED, wavelength: 454 nm, and irradiance: 6.5 mW cm^{-2}). Schematics of (D) the vapor-fed PEC system under visible light irradiation and (E) PEC water splitting with applied voltage, depicted as ΔE. Figures (A-D) were reproduced with permission from ref.[28], Copyright 2020, American Chemical Society.

During the vapor-fed process in a PEM-PEC cell with the porous WO_3/Mo-$BiVO_4$ heterojunction photoanode, H_2 was produced with an IPCE of 10% at 454 nm and 1.2 V under blue-light irradiation [Figure 9C and D]. This was achieved with an FE of approximately 100 and 94% for H_2 and O_2 generation, respectively. However, the H_2 production rate in PEM-PEC cells gradually decreased during light irradiation. One cause of this degradation is the photocorrosive dissolution of $BiVO_4$ under acidic conditions[40]. When using strongly acidic PEM or PFSA ionomers, it is crucial to consider the chemical stability of the semiconductor electrode materials, including the cocatalysts. Furthermore, a porous W-doped $BiVO_4$ photoanode demonstrated solar H_2 production from ambient air with humidity (RH: 100%) in the PEM-PEC reactor, retaining a current density of 1.55 mA·cm^{-2} at 1.23 V *vs.* RHE under AM1.5 simulated solar light[41]. For STH energy conversion, the applied voltage must be less than 1.23 V [Figure 9E]. Moreover, much research effort is needed for narrow-bandgap photoelectrodes with visible light absorption edges longer than 500 nm to increase STH efficiency.

CONCLUSION AND OUTLOOK

A PEM-PEC reaction system capable of operating in a gas-phase environment was successfully developed by engineering the triple-phase boundary of a "gas-electrolyte-semiconductor" interface. By utilizing porous photoelectrodes (for gas diffusion) with a surface coating of thin ionomer films (for enhanced proton conductivity), the photocurrent response of the semiconductor particles under vapor-feeding conditions was enhanced significantly. This triple-phase boundary facilitated the oxidative decomposition of the adsorbed water species through a proton-coupled electron transfer and proton transport, leading to O_2 production with a high FE. Concurrently, the H_2 produced at the cathode was separated from O_2 using a solid polymer electrolyte.

While the TiO_2 photoanode exhibited some oxidative degradation of the thin film of PFSA ionomer during the PEM-PEC reactions, the $SrTiO_3$ photoanode significantly improved the selectivity for O_2 generation and extended the long-term stability under gas-phase conditions. Additionally, the applied voltage was successfully reduced to 0.3 V by the use of the $SrTiO_3$ photoanode for overall water splitting. The introduction of a Mo-doped $BiVO_4$ layer on the WO_3 photoanode further enhanced its visible light responsivity. Although the STH conversion efficiency of the photoelectrode materials is still under development, further enhancements of the PEC performance are anticipated through applied voltage reduction and the broadening of the visible light response range by optimizing the preparation method for the porous photoelectrodes with narrow bandgap. To improve the PEC properties, the rational design of the structures and the composition, including p-n junction, heterojunction, doping, passivation layer, and cocatalyst loading, need to be further investigated. Research is also needed to understand the mechanism of proton conduction at low humidity and to efficiently capture low concentrations of water vapor in the outside air.

The gas-phase PEM-PEC system has the potential for applications beyond water vapor decomposition, including the activation of methane at around room temperature, where methane is converted to yield hydrogen and ethane as products[24,42]. Moreover, this system can be adapted to generate diverse energy carriers beyond hydrogen by modifying the type of electrocatalyst at the cathode. Porous p-type semiconductor electrodes, such as copper oxide (Cu_2O) and organic bulk heterojunctions, have been investigated for the PEM-PEC system[43,44]. The use of anion exchange membranes instead of PEM is also expected for specific materials and reactions. The approach introduced in this review is expected to find applications in other intriguing small-molecule conversion reactions, such as CO_2 reduction, NH_3 synthesis, H_2O_2 production, and H_2 generation.

DECLARATIONS

Authors' contributions

Conceptualization, data curation, visualization, writing - original draft preparation, and writing - review & editing: Amano F

Data curation and writing - original draft preparation: Tsushiro K

Availability of data and materials

Not applicable.

Financial support and sponsorship

This study was supported by the Japan Society for the Promotion of Science (JSPS), KAKENHI (grant number: JP20H02525).

Conflicts of interest

Both authors declared that there are no conflicts of interest.

Ethical approval and consent to participate

Not applicable.

Consent for publication

Not applicable.

REFERENCES

1. Hisatomi T, Domen K. Reaction systems for solar hydrogen production via water splitting with particulate semiconductor photocatalysts. *Nat Catal* 2019;2:387-99. DOI
2. Takata T, Domen K. Particulate photocatalysts for water splitting: recent advances and future prospects. *ACS Energy Lett* 2019;4:542-9. DOI
3. Kim JH, Hansora D, Sharma P, Jang JW, Lee JS. Toward practical solar hydrogen production - an artificial photosynthetic leaf-to-farm challenge. *Chem Soc Rev* 2019;48:1908-71. DOI PubMed
4. Yang W, Prabhakar RR, Tan J, Tilley SD, Moon J. Strategies for enhancing the photocurrent, photovoltage, and stability of photoelectrodes for photoelectrochemical water splitting. *Chem Soc Rev* 2019;48:4979-5015. DOI PubMed
5. Guo J, Zhang YC, Zavabeti A, et al. Hydrogen production from the air. *Nat Commun* 2022;13:5046. DOI PubMed PMC
6. Kumari S, Turner White R, Kumar B, Spurgeon JM. Solar hydrogen production from seawater vapor electrolysis. *Energy Environ Sci* 2016;9:1725-33. DOI
7. Lewis NS. Developing a scalable artificial photosynthesis technology through nanomaterials by design. *Nat Nanotechnol* 2016;11:1010-9. DOI PubMed
8. Chabi S, Papadantonakis KM, Lewis NS, Freund MS. Membranes for artificial photosynthesis. *Energy Environ Sci* 2017;10:1320-38. DOI
9. Suguro T, Kishimoto F, Takanabe K. Photocatalytic hydrogen production under water vapor feeding - a minireview. *Energy Fuels* 2022;36:8978-94. DOI
10. Dionigi F, Vesborg PCK, Pedersen T, et al. Gas phase photocatalytic water splitting with $Rh_{2-y}Cr_yO_3$/GaN:ZnO in μ-reactors. *Energy Environ Sci* 2011;4:2937-42. DOI
11. Daeneke T, Dahr N, Atkin P, et al. Surface water dependent properties of sulfur-rich molybdenum sulfides: electrolyteless gas phase water splitting. *ACS Nano* 2017;11:6782-94. DOI
12. Suguro T, Kishimoto F, Kariya N, et al. A hygroscopic nano-membrane coating achieves efficient vapor-fed photocatalytic water splitting. *Nat Commun* 2022;13:5698. DOI PubMed PMC
13. Amano F, Mukohara H, Sato H, Tateishi C, Sato H, Sugimoto T. Vapor-fed photoelectrolysis of water at 0.3 V using gas-diffusion photoanodes of $SrTiO_3$ layers. *Sustain Energy Fuels* 2020;4:1443-53. DOI
14. Spurgeon JM, Lewis NS. Proton exchange membrane electrolysis sustained by water vapor. *Energy Environ Sci* 2011;4:2993-8. DOI
15. Fujishima A, Honda K. Electrochemical photolysis of water at a semiconductor electrode. *Nature* 1972;238:37-8. DOI
16. Ichikawa S, Doi R. Hydrogen production from water and conversion of carbon dioxide to useful chemicals by room temperature photoelectrocatalysis. *Catal Today* 1996;27:271-7. DOI
17. Seger B, Kamat PV. Fuel cell geared in reverse: photocatalytic hydrogen production using a TiO_2/Nafion/Pt membrane assembly with no applied bias. *J Phys Chem C* 2009;113:18946-52. DOI
18. Li Y, Yu H, Song W, Li G, Yi B, Shao Z. A novel photoelectrochemical cell with self-organized TiO_2 nanotubes as photoanodes for hydrogen generation. *Int J Hydrogen Energy* 2011;36:14374-80. DOI
19. Rongé J, Nijs D, Kerkhofs S, Masschaele K, Martens JA. Chronoamperometric study of membrane electrode assembly operation in continuous flow photoelectrochemical water splitting. *Phys Chem Chem Phys* 2013;15:9315-25. DOI PubMed
20. Xu K, Chatzitakis A, Norby T. Solid-state photoelectrochemical cell with TiO_2 nanotubes for water splitting. *Photochem Photobiol Sci* 2017;16:10-6. DOI PubMed
21. Georgieva J, Armyanov S, Poulios I, Sotiropoulos S. An all-solid photoelectrochemical cell for the photooxidation of organic vapours under ultraviolet and visible light illumination. *Electrochem Commun* 2009;11:1643-6. DOI
22. Iwu KO, Galeckas A, Kuznetsov AY, Norby T. Solid-state photoelectrochemical H_2 generation with gaseous reactants. *Electrochim Acta* 2013;97:320-5. DOI
23. Rongé J, Deng S, Pulinthanathu Sree S, et al. Air-based photoelectrochemical cell capturing water molecules from ambient air for hydrogen production. *RSC Adv* 2014;4:29286-90. DOI
24. Amano F, Shintani A, Tsurui K, Mukohara H, Ohno T, Takenaka S. Photoelectrochemical homocoupling of methane under blue light irradiation. *ACS Energy Lett* 2019;4:502-7. DOI
25. Amano F, Shintani A, Mukohara H, Hwang YM, Tsurui K. Photoelectrochemical gas-electrolyte-solid phase boundary for hydrogen production from water vapor. *Front Chem* 2018;6:598. DOI PubMed PMC
26. Amano F, Mukohara H, Shintani A, Tsurui K. Solid polymer electrolyte-coated macroporous titania nanotube photoelectrode for gas-phase water splitting. *ChemSusChem* 2019;12:1925-30. DOI PubMed
27. Amano F, Mukohara H, Sato H, Ohno T. Photoelectrochemical water vapor splitting using an ionomer-coated rutile TiO_2 thin layer on titanium microfiber felt as an oxygen-evolving photoanode. *Sustain Energy Fuels* 2019;3:2048-55. DOI
28. Ta CXM, Akamoto C, Furusho Y, Amano F. A macroporous-structured WO_3/Mo-doped $BiVO_4$ photoanode for vapor-fed water splitting under visible light irradiation. *ACS Sustain Chem Eng* 2020;8:9456-63. DOI
29. Amano F, Shintani A, Tsurui K, Hwang YM. Fabrication of tungsten trioxide photoanode with titanium microfibers as a three

dimensional conductive back contact. *Mater Lett* 2017;199:68-71. DOI

30. Amano F, Koga S. Electrochemical impedance spectroscopy of WO_3 photoanodes on different conductive substrates: the interfacial charge transport between semiconductor particles and Ti surface. *J Electroanal Chem* 2022;921:116685. DOI
31. Homura H, Ohtani B, Abe R. Facile fabrication of photoanodes of tungsten(VI) oxide on carbon microfiber felts for efficient water oxidation under visible light. *Chem Lett* 2014;43:1195-7. DOI
32. Homura H, Tomita O, Higashi M, Abe R. Application of carbon microfiber felts as three-dimensional conductive substrate for efficient photoanodes of tungsten(VI) oxide. *J Photochem Photobiol A* 2019;375:54-63. DOI
33. Stoll T, Zafeiropoulos G, Tsampas MN. Solar fuel production in a novel polymeric electrolyte membrane photoelectrochemical (PEM-PEC) cell with a web of titania nanotube arrays as photoanode and gaseous reactants. *Int J Hydrog Energy* 2016;41:17807-17. DOI
34. Makarova MV, Amano F, Nomura S, et al. Direct electrochemical visualization of the orthogonal charge separation in anatase nanotube photoanodes for water splitting. *ACS Catal* 2022;12:1201-8. DOI
35. Zafeiropoulos G, Johnson H, Kinge S, van de Sanden MCM, Tsampas MN. Solar hydrogen generation from ambient humidity using functionalized porous photoanodes. *ACS Appl Mater Interfaces* 2019;11:41267-80. DOI PubMed
36. Zafeiropoulos G, Stoll T, Dogan I, Mamlouk M, van de Sanden M, Tsampas M. Porous titania photoelectrodes built on a Ti-web of microfibers for polymeric electrolyte membrane photoelectrochemical (PEM-PEC) cell applications. *Sol Energy Mater Sol Cells* 2018;180:184-95. DOI
37. Stoll T, Zafeiropoulos G, Dogan I, et al. Visible-light-promoted gas-phase water splitting using porous WO_3/$BiVO_4$ photoanodes. *Electrochem Commun* 2017;82:47-51. DOI
38. Xu K, Chatzitakis A, Vøllestad E, Ruan Q, Tang J, Norby T. Hydrogen from wet air and sunlight in a tandem photoelectrochemical cell. *Int J Hydrog Energy* 2019;44:587-93. DOI
39. Kang X, Chaperman L, Galeckas A, et al. Water vapor photoelectrolysis in a solid-state photoelectrochemical cell with TiO_2 nanotubes loaded with CdS and CdSe nanoparticles. *ACS Appl Mater Interfaces* 2021;13:46875-85. DOI
40. Ta CXM, Furusho Y, Amano F. Photoelectrochemical stability of WO_3/Mo-doped $BiVO_4$ heterojunctions on different conductive substrates in acidic and neutral media. *Appl Surf Sci* 2021;548:149251. DOI
41. Zafeiropoulos G, Varadhan P, Johnson H, et al. Rational design of photoelectrodes for the fully integrated polymer electrode membrane-photoelectrochemical water-splitting system: a case study of bismuth vanadate. *ACS Appl Energy Mater* 2021;4:9600-10. DOI
42. Amano F, Shintani A, Sakakura T, Takatsuji Y, Haruyama T. Photoelectrochemical C-H activation of methane to methyl radical at room temperature. *Catal Sci Technol* 2023;13:4640-5. DOI
43. Amano F, Uchiyama A, Furusho Y, Shintani A. Effect of conductive substrate on the photoelectrochemical properties of Cu_2O film electrodes for methyl viologen reduction. *J Photochem Photobiol A* 2020;389:112254. DOI
44. Caretti M, Mensi E, Kessler RA, et al. Transparent porous conductive substrates for gas-phase photoelectrochemical hydrogen production. *Adv Mater* 2023;35:e2208740. DOI